ANATOMIA HISTOLOGIA EMBRYOLOGIA
JOURNAL OF VETERINARY MEDICINE

Anat. Histol. Embryol.
ISSN 0340–2096

doi: 10.1111/j.1439-0264.2009.00973.x

Orthopaedic Clinic University of Brescia, Brescia, Italy

Morphometric Analysis of the Canal System of Cortical Bone: An Experimental Study in the Rabbit Femur Carried Out with Standard Histology and Micro-CT

U. E. Pazzaglia[1]*, G. Zarattini[1], D. Giacomini[2], L. Rodella[3], A. M. Menti[2] and G. Feltrin[2]

Addresses of authors: [1]Orthopaedic Clinic, University of Brescia, Brescia, Italy; [2]Department of Medical-Diagnostic Sciences and Special Therapies, University of Padua, Sezione di Radiologia, Padua, Italy; [3]Department of Human Anatomy, University of Brescia, Brescia, Italy; *Corresponding author: Tel.: +390303995401; fax: +39030397365; e-mail: ortopedia2@spedalicivili.brescia.it

With 11 figures and 1 table

Received May 2009; accepted for publication August 2009

Summary

The osteonal pattern of cortical bone is gradually built around the intracortical vessels by the progression of the cutting cones (secondary remodelling); therefore, the central canal size can be used as index of the remodelling activity. An experimental model in the rabbit femur was used to investigate, through central canal morphometry and frequency distribution analysis, the remodelling activity, comparing the middle of the diaphysis (mid-shaft) with the extremity (distal-shaft) and at the same level sectors and layers of the cortex in transversal sections. The study documented a higher density of canals in the mid-shaft than in the distal-shaft and a higher remodelling in the distal-shaft. There were no significant differences between dorsal, ventral, medial and lateral sectors at both mid-shaft and distal-shaft levels, while the number of canals was higher in the sub-periosteal layers than in the sub-endosteal. A lower threshold of 40 μm^2 was observed in the central canal area. Sealed osteons in the midshaft were 22.43% of the total number of osteons of the central canal area between 40 and 200 μm^2 and 0.44% of those of the distal-shaft. Micro-CT allowed a 3D reconstruction of the vascular canal system, which confirmed the branched network pattern rather than the trim architecture of the traditional representation. Some aspects like the lower threshold of the central canal size and the sealed osteons documented the plasticity of the system and its capacity for adaptation to changes in the haemodynamic conditions.

Introduction

The Haversian systems of the diaphyseal bone are built around the intracortical vessels and their organization advances simultaneously with the vascular network development (Lee et al., 1965; Harris et al.,1968); therefore, the intracortical canals reproduce the same design of the vessels network. The size of the osteon central canal can be correlated with its age in the early phase of its maturation (Smith, 1960, 1963) because the internal organization of cutting cones is characterized by the concentrical lamellar apposition behind the advancing head (Schenk et al., 1964). The other lamellar systems of the cortical bone present on the endosteal and periosteal surfaces of the diaphysis (Smith, 1960; Hert and Hladikova, 1961; Albu et al., 1973) are also subjected to secondary remodelling when the bone broadens its perimeters during growth.

Even if the intracortical canal system is more accurately represented by a network model (Pazzaglia et al., 2008, 2009), there is a prevailing orientation of the Haversian canals along the axis of the shaft (Hert et al., 1994; Cohen and Harris, 1958; Vasciaveo & Bartoli, 1961) allowing a morphometric approach to the study of secondary remodelling (Martin et al., 1980; Barth et al., 1992; Feik et al., 1997).

In the present study, analysis was carried out by counting the number of osteons in transversal sections of the diaphysis and measuring the central canals area. These data were compared between different levels (mid-shaft and distal-shaft), sectors (ventral, dorsal, medial and lateral) and layers of the cortex. The investigation was extended to the 3D morphology of the diaphyseal cortical bone with micro-CT, assessing the tissue and canal volumes, the cortical porosity, the canal surface and the canal shape morphology. These data contribute to the knowledge of the cortical bone architecture using a model that differs from the traditional representation (Thompson, 2002).

Materials and Methods

The study was carried out on the femurs of six male New Zealand white rabbits approximately aged 8 months (Stefano Morini, S. Polo d'Enza, Reggio Emilia, Italy) with a body weight between 2.5 and 3 kg. The animals were housed in individual cages with free access to food and water and kept in an animal facility at a constant temperature of 22°C with 12 h light-dark cycle. Care and use of experimental animals were consistent with procedures and regulations of the Italian Health Ministry.

The rabbits were euthanized with an overdose of ketamine cloridrate (Imagel; Mevial Italia SpA, Assago (Mi), Italy) and xylazine (Rompum; Bayer AG, Leverkusen, Germany).

The right femurs, after fixation in neutral formalin solution (10%), were decalcified in Osteosoft (Merck S.p.a., Milan, Italy) at 37°C for 2 months. The bones were cut with a blade in a plane perpendicular to the major axis of the bone at the mid-length: the proximal part of the femurs was discarded; the remaining part was further split cutting out the epiphyses and part of the metaphyses (with a section about 2 mm below the distal growth plate cartilage). Two cylinders, about 6–7 mm in length, were obtained from the extremities of these specimens, the first including the distal metaphysis and the adjoining diaphysis, marked as distal-shaft, the second corresponding to

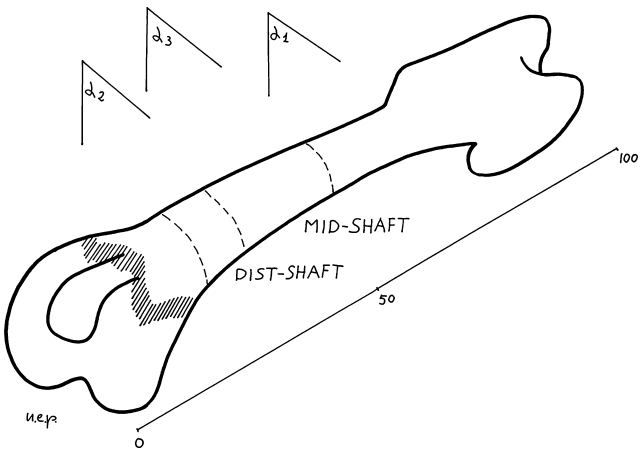

Fig. 1. Schema of the femur showing the transversal cut levels used to define mid-shaft and distal-shaft.

the mid-diaphysis, marked as mid-shaft (Fig. 1). These specimens were then processed and embedded vertically in paraffin blocks. Serial sections about 10 μm thick were cut with the microtome in the plane perpendicular to the long axis of the bone. They were stained with haematoxylin-eosin and the best (without technical artefacts) 20 slides representative of all the levels of the cylinder were selected for morphometry. The slides were examined using an Olympus BX51 microscope in bright field, in polarized light and in phase contrast.

The left femurs were fixed in neutral formalin solution in the same way and the mid-shaft segment corresponding to the right femur was transversely cut using a low-speed diamond saw (Isomet; Buheler Ltd, Lake Placid, NY, USA). These specimens were then transferred to a bath of 40% hydrogen peroxide solution in water at room temperature for 4 weeks to remove all soft tissues without damaging the bone and then air-dried at room temperature for 48 h. These specimens had the shape of a cylinder about 1.5 cm high; they were split in the longitudinal plane with further cuts and the segment corresponding to the dorsal cortex was reduced to a bar about 2 mm in diameter, with intact endosteal and periosteal surfaces. One bar from each rabbit's left femur was examined with micro-CT.

Morphometry

Digital images of the right femur decalcified sections corresponding to mid-shaft and distal-shaft were captured using a Colorview IIIu camera mounted on a Olympus BX51 microscope. Utilizing the software Cell (Soft Imaging System GmbH, Munster, Germany), the cortical area was measured and the number of vascular canals was counted and expressed as a function of the cortical area (n/mm^2). The area of the canals was measured as later reported and the frequency distribution for area classes was calculated.

On the same transversal sections, four sectors were designed according to the following criteria:

1. The a-p (vertical) and lateral (horizontal) axes of the section were traced intersecting in a point indicated as the centre of the section (C).
2. Through the point C, two lines were traced forming with the vertical and horizontal axes two angles of 60° and 30° respectively.
3. The intersections of these lines with the endosteal and periosteal perimeters were used to identify four sectors of the cortex, marked as ventral, dorsal, medial and lateral. In each sector, four microscopic fields were selected, at 40× enlargement, which included the full thickness of the cortex between the endosteal and the periosteal surface: the fields were regularly distributed along the perimeter of the sector and their total area represented approximately three-fourths of the entire surface of that sector (Fig. 2). The cortical area of each sector was therefore represented by the sum of the areas of the fields of each sector and the number of canals expressed as function of this area (canals density). The area of the canals in each sector was measured utilizing a function of the programme which discriminates the empty surface (white) from the stained matrix. When cell or stain deposits inside the individual canals made the automatic measurement application impossible, the canal perimeter was manually traced utilizing the zoom function and the area was consequently evaluated. Those canals intersected by the margins of the microscopic fields or those in which the canal was twice or more as long in one direction than in the other were considered not to be running perpendicularly to the plane of section and disqualified (Jowsey, 1966).

The area of each canal was assigned to one of nine classes of 200 μm^2 each, with the exception of the last, which included values over 1600 μm^2. Histograms representing the frequency distribution for area classes in each section and sector were then plotted comparing mid-shaft versus distal-shaft and the four sectors at levels of mid-shaft and distal-shaft. The values of these parameters for each rabbit mid-shaft and distal-shaft of the femur were the mean of 20 serial slides.

The dorsal and ventral sectors of each mid-shaft section were further divided into five layers of equal thickness: the outer and inner one-fifth were marked respectively as sub-periosteal and sub-endosteal; the remaining central three-fifths were indicated as middle cortex (Fig. 3a,b). The area of each layer, the density of canals and the frequency distribution for area classes were compared between full sections and the

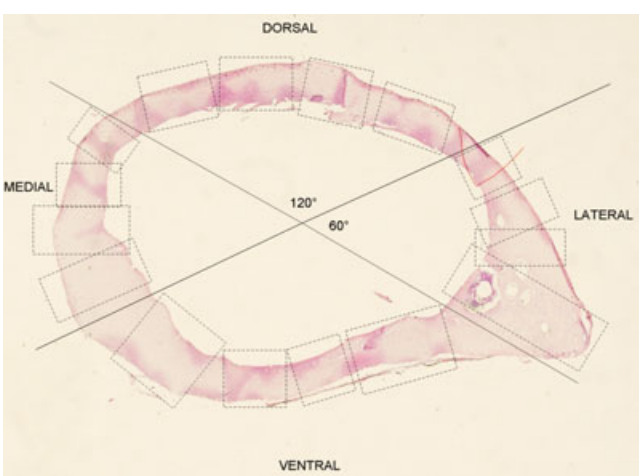

Fig. 2. Haematoxylin-eosin (1.5×) mid-shaft transversal sections with lines used to define dorsal, ventral and medial sectors. Dotted rectangles indicate the microscopic fields used for morphometric evaluation of each sector.

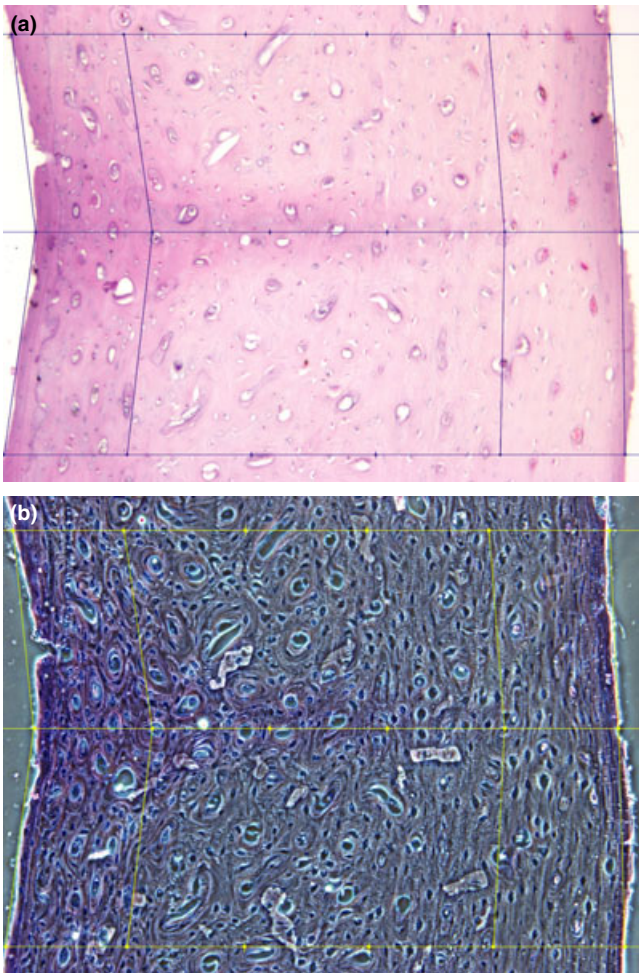

Fig. 3. (a) Haematoxylin-eosin (40×) mid-shaft transversal section with lines used to define sub-periosteal, middle cortex and sub-endosteal layers respectively 1/5, 3/5 and 1/5 of the total cortex thickness. (b) The same field in phase-contrast.

sectors. The canals intersected by margins of sectors and layers were excluded from evaluation as well as those with a ratio between the major and minor diameters of the ellipsoid over 2:1.

A separate evaluation at a higher enlargement (200×) was carried out on the whole mid- and distal-shaft sections to analyse the lower limit of canal size. A grid of points forming a 0.5-mm^2-mesh net was adhered to the glass coverslip; these points served as marks to select the microscopic fields at the 200× enlargement in such a way that they were regularly distributed on the whole surface of the tissue section. On each slide, according to its area, 40–50 fields were evaluated. In each field, the areas of all class 1 canals (0–200 μm^2) were measured and distributed in ten sub-classes of 20 μm^2 each: the frequency distribution for the 20 μm^2 sub-classes was calculated in both the mid-shaft and the distal-shaft.

Micro-CT

The specimens were examined using a Skyscan 1172 HR micro-CT (Skyscan, Aartselaar, Belgium) after vertical positioning in the cylindrical polyethylene container. The scanning protocol included: 80 kV voltage, 124 μA of current, 2904 ms of exposure time, filter of aluminium with a 1 mm thickness to reduce the beam-hardening artefact, 1280 × 1024 pixel of field of view, 3 μm of isotropic voxel size. The protocol included a sample's rotation through 360°, with single step of 0.4°. A six-frame average was used to improve the signal-to-noise ratio. The row data acquired were reconstructed using N-RECON software (Skyscan), which uses the beck-projection algorithm to reconstruct axial subsequent images saved in bitmap format. This facilitated efficient manipulation of the large data sets while still providing resolution sufficient to visualize intracortical canals. Tissue volume (TV), canal volume (CaV), cortical porosity (CaV/TV) and canal surface (CS) were calculated in each femur and expressed as mean ± standard deviation.

The serial image data sets of each femur were manually screened for longitudinal canals: to be chosen, a longitudinal canal had to have a ratio between the major and minor diameter not greater than 2:1. The length of the canal examined was that between two consecutive branches. For each canal identified in this way, the volume of the empty space was digitally excised, using the program CTAn (Skyscan), from the larger image data sets and resampled to generate serial transversal sections. These were carried out with the same direction from proximal to distal along the whole length of the canal and the corresponding circumference was measured. The circumference variations were expressed in a graph, reporting in abscissa the values measured and in ordinate the sequence of the section planes from proximal to distal. A total of 222 canals in six femurs with a mean thickness of 30.6 μm, distributed in the six femur specimens, were studied.

Statistical analysis

In the decalcified sections of the right femurs, the total cortical area, the density of vascular canals and the frequency distribution for area classes in the cortex of mid-shaft and distal-shaft were compared with a paired Student's t-test and a Pearson chi-squared test respectively.

The density of vascular canals and the frequency distribution for area classes were compared among dorsal, ventral, medial and lateral sectors of the mid-shaft and distal-shaft using analysis of variance and Pearson chi-squared tests.

In the mid-shaft dorsal and ventral sectors, the difference in the same parameters was evaluated among sub-periosteal, middle and sub-endosteal layers.

The values of these parameters for each rabbit were the mean of 20 serial slides of the femur mid-shaft and distal-shaft.

Results

The transversal sections of the cortical bone at mid-shaft level had an approximate ellipsoidal shape with the lateral diameter larger than the antero-posterior. The thickness of the cortex was not uniform, with the medial and lateral sectors more irregular and larger than the dorsal and the ventral. The lateral sector presented a crest with four to six very large vascular spaces inside (Fig. 2). The distal-shaft sections were circular, with the cortex thickness more regular and without the lateral crest. The vascular canals density was higher ($P < 0.001$) in the mid-shaft than in distal-shaft. No significant differences in the mean vascular canals density was observed among dorsal,

ventral, medial and lateral sectors of both mid-shaft and distal-shaft or between dorsal and ventral mid-shaft layers (Table 1).

The frequency distribution of vascular canals for 200 μm^2 area classes showed in classes 1 and 2 a higher number of canals in the mid-shaft than in the distal-shaft, while in classes 4–9, the number of canals was significantly higher in the distal-shaft (Fig. 4). There were no significant differences in canals area distribution between sectors of the mid-shaft (Fig. 5a) and of the distal-shaft (Fig. 5b).

The higher number of canals in the middle cortex layer was determined by the geometrical criteria of layers selection. In class 1 of both dorsal and ventral sectors, a significantly higher number of canals were observed in the sub-periosteal layer than in the corresponding sub-endosteal layer. The comparison of these layers in all the other classes was not significant. Comparing the corresponding classes and layers of dorsal and ventral sectors, there was a significant higher number of canals in dorsal middle-cortex layers of class 1 and 2 and in dorsal sub-periosteal layer of class 1 (Fig. 6a,b).

A lower threshold of 40 μm^2 of the osteon central canal area was documented extending the analysis of the frequency distribution of class 1 canals into sub-classes of 20 μm^2 area (Fig. 7). Osteons with the central canal occluded by bone matrix were regularly observed: the lumen of the central canal was delimited by an eosinophilic line, similar in this respect to the reversal line, but otherwise not crenulated (Fig. 8a) and an osteocytic lacuna with its own cell could be observed either in central or in eccentric position. High enlargement observation in phase contrast (Fig. 8b) and in polarized light of the material sealing the canal documented the lamellar pattern of this material. The sealed osteons in the mid-shaft were 22.43% of all osteons with a central canal area within 200 μm^2, in the distal-shaft they were 0.44%. With micro-CT, the canal volume/tissue volume (CT/CV), the canal surface density (CS/TV) and the canal thickness were analysed for the volume of mid-shaft examined (Fig. 9) and it allowed a 3-D reconstruction of the vascular canals system documenting a network pattern with a prevailing longitudinal polarization (Fig. 10). The analysis of circumference variations in the sequence of micro-CT cuts of individual osteons produced the following five canal shape types: (i) cylindrical (39.2%); (ii) conical proximally opened (9.4%); (iii) conical distally opened (35.1%); (iv) ellipsoidal (12.2%); (v) hyperbolical (4.1%) (Fig. 11).

Discussion

The cortical bone is currently presented as a set of geometrical modules aggregated in three lamellar systems, the periosteal, the endosteal and the Haversian (Hert and Hladikova, 1961; Smith, 1960), the latter with straight, longitudinal canals (Havers') and transversal connections (Volkmann's). The trim architecture of the Haversian system is often advocated to support the theories on mechanical determination of the bone structure (Lanyon and Baggott, 1976; Frost, 1979; Lanyon and Bourn, 1979). The morphological and morphometric approach of this study questions the currently accepted model of the cortical bone architecture (Ham, 1952; Thompson, 2002).

The precision of measurement of the cortical canals circumference or area is conditioned by the plane of the histological section. There is a large body of evidence that the canals of the secondary osteonal system in the diaphysis are oriented in a direction approximately parallel to the longitudinal axis (Stout et al., 1999; Mohsin et al., 2002; Trias & Fery, 1979); therefore, transversal sections can be assumed to be perpendicular or near perpendicular to the axis of the Haversian canals. The limiting criterion to exclude from the size assessment those canals with a ratio major/minor diameter over 2:1 has been already adopted in morphometric studies of the bone (Jowsey et al., 1965; Jowsey, 1966) and it proved to

Table 1. Mean cortex area and density of vascular canals in mid-shaft and distal-shaft of the rabbit right femur ($P < 0.05$)

	Right distal femur ($n = 6$)	
	Mid-shaft	Distal-shaft
Cortex area (mm^2)	15.39 ± 0.296	17.22 ± 1.443
Vascular canals density (n/mm^2)	111.3 ± 14.48	58.87 ± 16.93

	Mid-shaft ($n = 6$)			
	Dorsal	Ventral	Medial	Lateral
Canals density (n/mm^2)	126.2 ± 42.49	104.4 ± 8.51	122.6 ± 37.4	97.9 ± 23.69

	Distal-shaft ($n = 6$)			
	Dorsal	Ventral	Medial	Lateral
Canals density (n/mm^2)	57.38 ± 11.61	52.8 ± 4.83	57.94 ± 5.75	54.79 ± 5.14

	Mid-shaft					
	Dorsal ($n = 6$)			VENTRAL ($n = 6$)		
	Sub-per.	Middle	Sub-end.	Sub-per.	Middle	Sub-end.
Canals density (n/mm^2)	144.9 ± 45.16	127.5 ± 37.8	111.4 ± 11.42	125.1 ± 13.43	105.5 ± 13.2	87.82 ± 46.98

Comparison of the mean density of canals between sectors (dorsal, ventral, medial and lateral) of mid-shaft and distal-shaft and between layers of mid-shaft dorsal and ventral sectors.

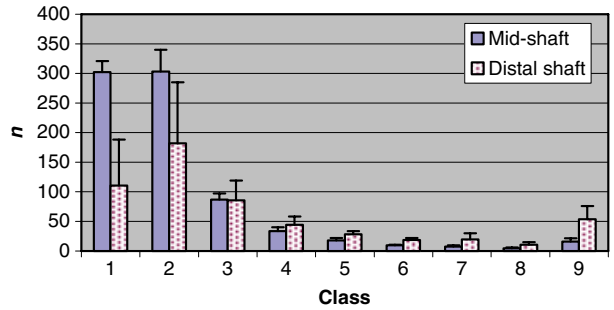

Fig. 4. Frequency distribution for 200 μ^2 area classes of canals in mid-shaft and distal-shaft of the femur in rabbits.

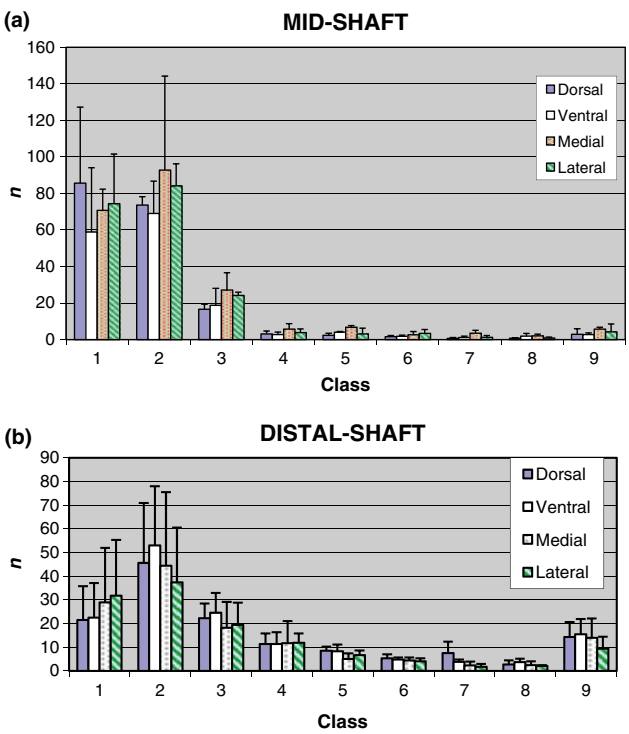

Fig. 5. (a, b) Frequency distribution for 200 μ^2 area classes of canals in dorsal, ventral, medial and lateral sectors of the mid-shaft (a) and distal-shaft (b).

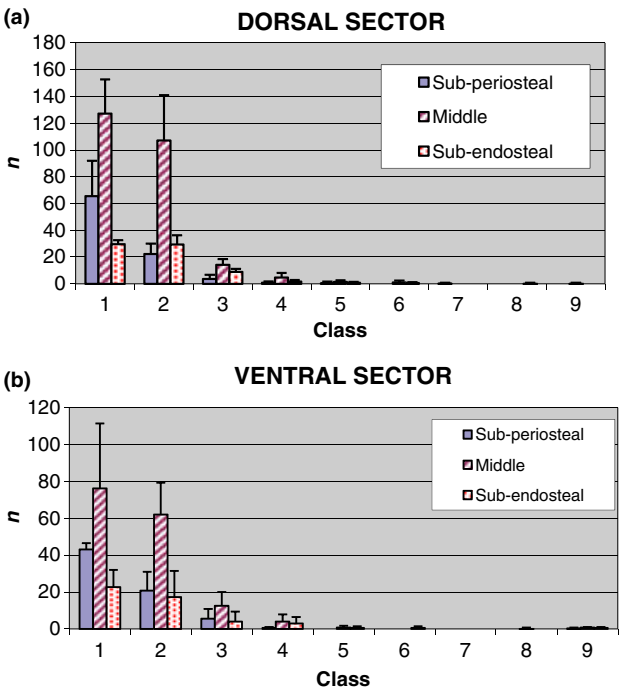

Fig. 6. (a, b) Frequency distribution for 200 μ^2 area classes of canals in sub-periosteal, middle cortex and sub-endosteal layers of the mid-shaft dorsal (a) and ventral (b) sectors.

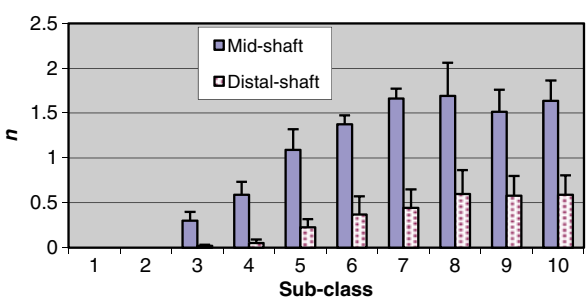

Fig. 7. Frequency distribution for 20 μ^2 area sub-classes of class 1 canals in mid-shaft and distal-shaft of the right femur in rabbits.

be useful to exclude those canals lying in transversal or oblique planes. Considering a geometric model consisting of a regular, vertical canal with a round section tilting of 30° produces a sectional area increment of 12.5% (Pazzaglia et al., 2007). As the deviations of secondary canals documented in 3D reconstruction of the canals cortical system have resulted well below this angle (Mohsin et al., 2002; Stout et al., 1999; Cohen and Harris, 1958; Cooper et al., 2006), the 12.5% variation of the central canal area can be assumed as the largest variation because of a defect of the specimen orientation.

A further bias of the morphometric assessment analysed with the frequency distribution for canal area classes is that not only completely structured secondary osteons (Havers') but also periosteal-derived canals are included. This lowers the sensitivity of the index, but does not invalidate its significance if differences are documented between levels, sectors or layers of the same bone, because canals of large area classes pertain exclusively to secondary remodelling. Equivalent cortex areas in distal-shaft and mid-shaft corresponded to a significant increment of the canals' density in the latter. These data are in agreement with the acknowledged model of bone growth with new bone added at the extremities of the diaphysis and accompanied by the advancement of new vessels, which enter inside the cortex from either the outer or inner surface of the metaphysis (Rogers and Gladstone, 1950; Brookes, 1963; Brookes and Revell, 1998). The Haversian canals with their longitudinal polarization and advancement trajectory contribute to the higher density at the mid-level of the diaphysis because the canals from the proximal and those from distal metaphyses intercalate at this level (Pazzaglia et al., 2008). A wide canal area corresponds to tunnels recently dug by cutting cones and the size of the central space results from the size of the original tunnel and by the number and thickness of the concentrical lamellae laid down by the osteoblasts (actually structuring secondary osteons); therefore, the analysis of canals frequency distribution for area classes confirms the

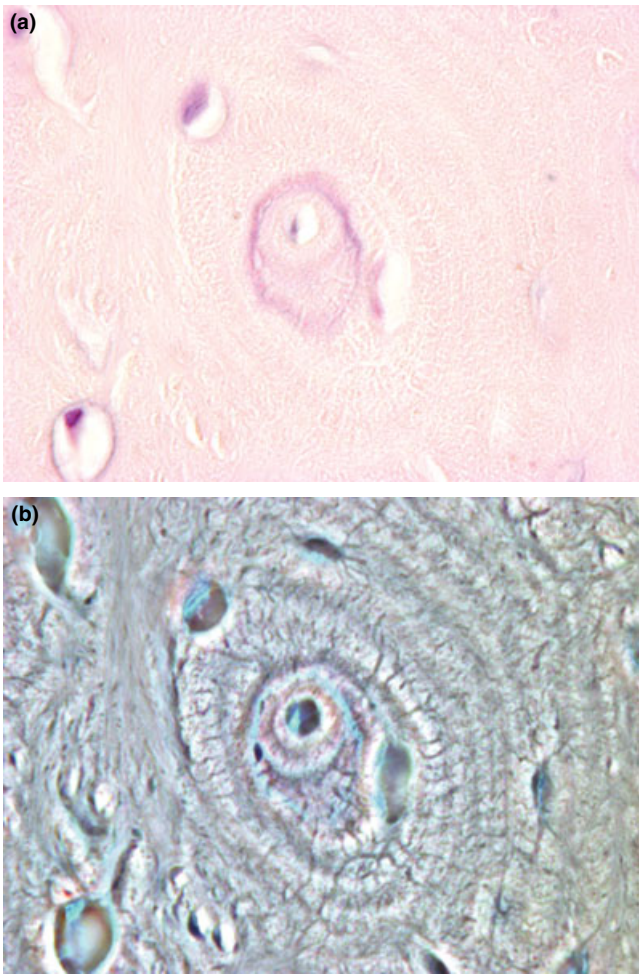

Fig. 8. (a) Haematoxylin-eosin (1000×). Aspect of sealed canals: the original lumen is delimited by a cement line and the occluding material has the same stain features of the bone matrix. (b) The same field in phase-contrast shows the fibrillar pattern of the material, not different from that of the outer lamellae.

Canal volume/Tissue volume	%	CT/TV	5.884 ±2.21
Canal surface density	1/μm	CS/TV	0.010±0.003
Canal thickness	μm	C.Th	30.56±9.91
Canal trabecular pattern factor	1/μm	C.Tb.Pf	0.109±0.028

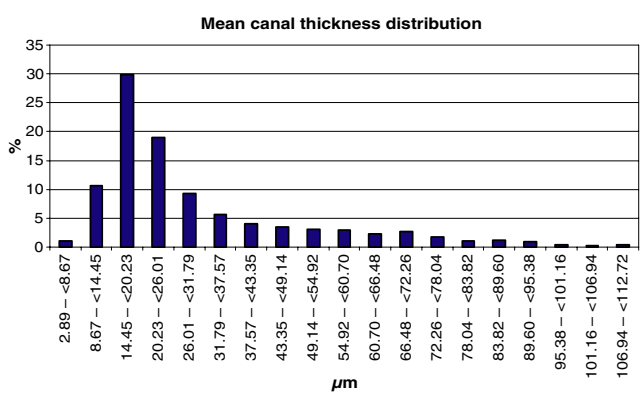

Fig. 9. Canal volume/tissue volume, canal surface density, canal thickness, canal trabecular pattern factor and mean canal thickness distribution determined in micro-CT.

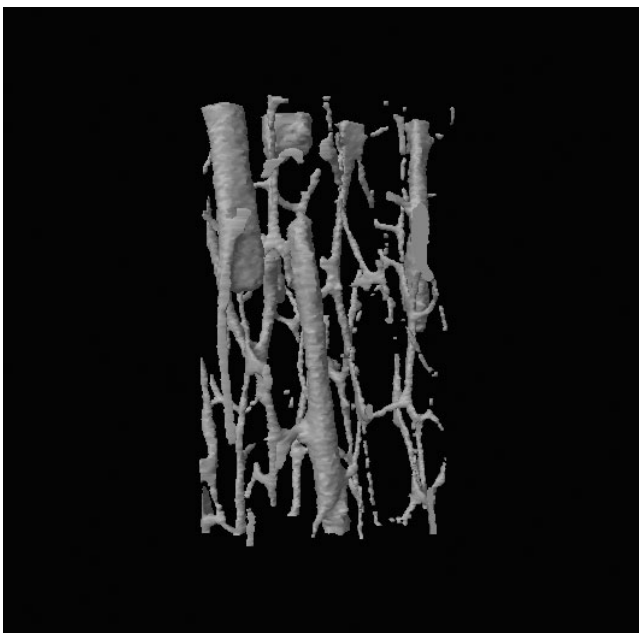

Fig. 10. Micro-CT reconstruction of the canal network in the volume of bone examined.

higher remodelling rate in the distal-shaft than in the mid-shaft (classes 4–9), while in classes 1 and 2, the higher number of small area canals in the mid-shaft is determined by the secondary osteons, which have completed their concentrical, lamellar structure (completely structured secondary osteons) and by the primary osteons. The latter are formed by incorporation of the periosteal vessels network and their central canal area is already determined by the size of the vessel (or vessels when more than one are incorporated inside a single canal). They are in the same size range of completely structured secondary osteons as soon as they are formed because around them, there is no concentric lamella apposition (Filogamo, 1946; Ham, 1952).

There are no significant differences in the distribution of actual structuring osteons between sectors of both mid-shaft and distal-shaft, indicating a well-balanced remodelling along the whole ring of the femoral cortex where no torsion or bending takes place in this stage of the bone development. The higher number of class 1 canals in the sub-periosteal layer than the number in the sub-endosteal can be explained by the addition of periosteal-derived canals (primary osteons) to the completely structured secondary osteons. The former are not present in the sub-endosteal layer where surface resorption is prevailing and even at those sites where apposition is present, it has the aspect of parallel lamellae without incorporation of vessels.

Histomorphometric analysis on compact bone transversal sections has been applied already to investigate the significance of the remodelling space (Dhem, 1978; Richman et al., 1979; Martin et al., 1980); Georgia et al., 1982; however, these studies addressed different species, or race and age variations in humans, which reduces the precision of the determination and makes the method not sufficiently accurate (Dhem, 1978). On the contrary, in this study, comparisons were performed within the same bone and the canal size analysis resulted in a reliable method to document the distribution of bone remod-

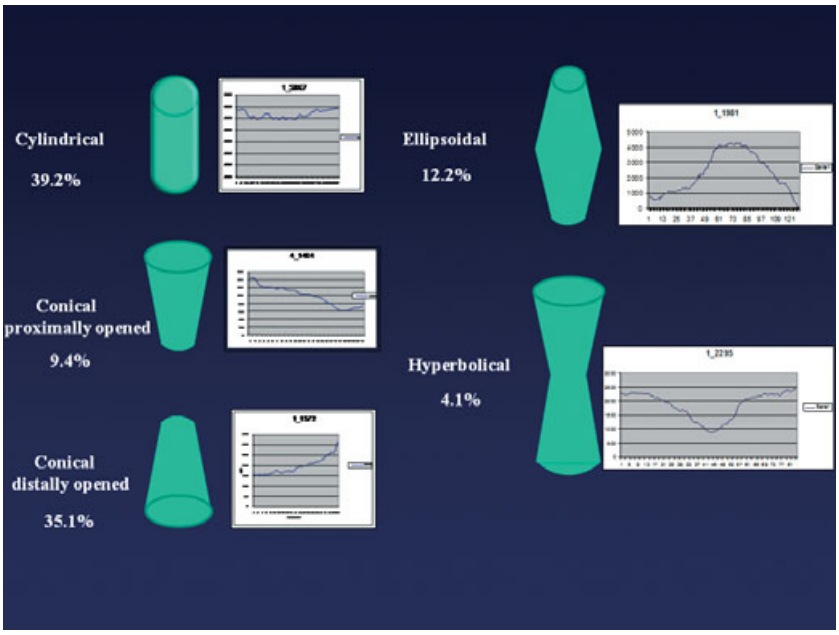

Fig. 11. Canal shape types according to the circumference variations in the sequence of micro-CT cuts of individual osteons.

elling in macro-areas of the cortex of a single bone and applicable to study the shape modelling of bones during growth and development. Using fluorescent-labelled Beagle dog ribs, significant differences of bone remodelling rates were documented along the length of the rib (Anderson & Danylchuk, 1978).

The histomorphometric analysis evidenced two further structural aspects of the diaphyseal cortical bone which, to the best of our knowledge, have previously not been investigated:

1. The lower threshold of 40 μm^2 for the central canal area of osteons suggests that the concentrical lamellar apposition inside haversian canals (also reported with the term 'radial rate of osteon closure' (Ilnicky et al., 1966; Polig and Jee, 1990) stops when the innermost lamellae get close to the central vessel wall; therefore, the calibre of the capillary-like vessel inside the canal seems to be the factor limiting the size of the secondary osteon central canal. This threshold is similar to that of primary osteons, with the exception of those containing more than one vessel.
2. Intact osteons with a sealed, central canal, which have been described as an occasional finding (Cohen and Harris, 1958), but no frequency data or a satisfactory explanation of their relationship with the intracortical vessels network have been reported and how or why they form. In this study, it was determined that there was a 22.43% incidence of sealed canals at level of the mid-shaft, which corresponded to the older and more remodelled level of the diaphysis, while they represented a rare and occasional observation in the distal-shaft. The possibility that these aspects could be technical artefacts must be kept in mind and certainly further investigations are warranted; however, the observation in polarized light at high power and in phase contrast of an organized fibrillar material with the same aspects of the osteonal lamellae within the space normally occupied by the vessel supports the hypothesis that this matrix has been produced by the same cells which apposed the concentrical lamellae of the osteon.

The morphology of the sealed osteon suggests a renewal of matrix apposition activity inside the central canal of a primary or a secondary osteon: collapse and degeneration of the vascular structure are the necessary conditions, because the sealing material fills the space within the inner resting line of the osteon in the place normally occupied by the central vessel. This explanation is coherent with a dynamic model of the intracortical circulation controlled by external factors like the pressure and flow inside the marrow and the periosteal arteries (Stein et al., 1958; Michelsen, 1967; Shim et al., 1972; Brinker et al., 1990). Any change in the intracortical flow direction and the adaptation to new flow dynamics may shut out a branch of the network from circulation: if this occurs, the excluded vessel wall collapses and the resting osteoblasts on the inner surface of the canal can renew matrix apposition.

There is no discrepancy between the observed threshold of the central canal size and the relatively high density of sealed osteons in the mid-shaft, because occlusion can occur in a short time, while the count of the sealed osteons is a figure referred to a much longer time interval, corresponding to the whole remodelling history of that level of bone.

The 3D reconstruction by micro-CT indicated the complex pattern of organization of the intracortical canals with frequent branching and the prevailing longitudinal orientation of the network (Cooper et al., 2003, 2007) in agreement with reconstructions carried out on serial sections of cortical bone (Stout et al., 1999; Mohsin et al., 2002). The cylindrical shape type canals correspond to primary osteons or to secondary osteons, which have completed their lamellar apposition (completely structured secondary osteons); the conical shape types to tunnels more recently dug and the opening of the cone corresponds to the advancement direction of the cutting cone; ellipsoidal and hyperbolical shapes are inconsistent with

conventional views on cortical remodelling and have been considered as irregular resorption spaces (Cooper et al., 2006).

Acknowledgements

The study was supported by research funds of Brescia University. Histological studies were carried out in labs of Brescia University, micro-CT on bone specimens was carried out by the Radiology Section of Padova University.

References

Albu, I., R. Georgia, E. Stoica, T. Giurgiu, and V. Pop, 1973: Le système des canaux de la couche compacte diaphysaire des os longs chez l'homme. Acta Anat. **84,** 43–51.

Anderson, C., and K. D. Danylchuck, 1978: Bone-remodelling rates of the Beagle: a comparison between different sites on the same rib. Am. J. Vet. Res. **39,** 1763–1765.

Barth, R. W., J. L. Williams, and F. S. Kaplan, 1992: Osteon morphometry in females with femoral neck fractures. Clin. Orthop. Relat. Res. **283,** 178–186.

Brinker, M. R., H. L. Lippton, S. D. Cook, and A. L. Hyman, 1990: Pharmacological regulation of the circulation of bone. J. Bone Joint Surg. Am. **72A,** 964–975.

Brookes, M., 1963: Cortical vascularization and growth in foetal tubular bones. J. Anat. **97,** 597–609.

Brookes, M., and W. L. Revell, 1998: Blood Supply of Bone. Scientific Aspects. London: Springer Verlag.

Cohen, J., and W. Harris, 1958: The three-dimensional anathomy of Haversian systems. J. Bone Joint Surg. Am. **40A,** 419–434.

Cooper, D. M., A. L. Turinsky, C. W. Sensen, and B. Hallgrimsson, 2003: Quantitative 3D analysis of the canal network in cortical bone by micro-computed tomography. Anat. Rec. B. **274,** 169–179.

Cooper, D. M., C. D. Thomas, J. C. Clement, and B. Hallgrimsson, 2006: Three-dimensional microcomputed tomography imaging of basic multicellular unit-related resorption spaces in human cortical bone. Anat. Rec. A. **288,** 806–816.

Cooper, D. M., C. D. Thomas, J. C. Clement, A. L. Turinsky, C. W. Sensen, and B. Hallgrimsson, 2007: Age-dependent change in the 3D structure of cortical porosity of the human femoral mid shaft. Bone **40,** 957–965.

Dhem, A., 1978: Significance of the haversian number. Bull. Assoc. Anat. (Nancy) **62,** 411–417.

Feik, S. A., C. D. Thomas, and J. G. Clement, 1997: Age-related changes in cortical porosity of the midshaft of the human femur. J. Anat. **191,** 407–416.

Filogamo, G., 1946: La forme e la taile des osteons chez quelques mammiferes. Arch. Biol. **57,** 137–143.

Frost, H. M., 1979: A chondral modelling theory. Calcif. Tissue Int. **28,** 181–200.

Georgia, R., I. Albu, M. Sicoe, and M. Georoceanu, 1982: Comparative aspects of the density and diameter of Haversian canals in the diaphyseal compact bone of man and dog. Morphol. Embryol. (Bucur) **28,** 11–14.

Ham, A. W., 1952: Some histophysiological problems peculiar to calcified tissues. J. Bone Joint Surg. Am. **24-A-3,** 701–728.

Harris, W. H., E. A. Haywood, J. Lavorgna, and D. Hamblen, 1968: Spatial and temporal variations in cortical bone formation in dogs. J. Bone Joint Surg. **50A,** 1118–1128.

Hert, J., and J. Hladikova, 1961: Die gefassversorgung des haversschen knochens. Acta Anat. **45,** 344–361.

Hert, J., P. Fiala, and M. Petrtyl, 1994: Osteon orientation of the diaphysis of the long bones in man. Bone **15,** 269–277.

Ilnicky, L., B. N. Epker, H. M. Frost, and R. Hattner, 1966: The radial rate of osteon closure evaluated by means of in vivo tetracycline labeling in beagle dog rib. J. Lab. Clin. Med. **67,** 447–454.

Jowsey, J., 1966: Studies of Haversian system in man and some animals. J. Anat. **100,** 857–864.

Jowsey, J., D. Phil, P. J. Kelly, B. L. Riggs, A. J. Bianco Jr, D. A. Scholz, and J. Gerson-Cohen, 1965: Quantitative microradiographic studies of normal and osteoporotic bone. J. Bone Joint Surg. Am. **47,** 785–806.

Lanyon, L. E., and D. G. Baggott, 1976: Mechanical function as an influence on the structure and form of bone. J. Bone Joint Surg. Br. **58,** 436–443.

Lanyon, L. E., and S. Bourn, 1979: The influence of mechanical function on the development and remodeling of the tibia An experimental study in sheep. J. Bone Joint Surg. Am. **61,** 263–273.

Lee, W. R., J. H. Marshall, and H. A. Sissons, 1965: Calcium accretion and bone formation in dogs. An experimental comparison between the results of Ca-45 kinetic analysis and tetracycline labelling. J. Bone Joint Surg. Br. **47,** 157–180.

Martin, R. B., J. C. Picket, and S. Zinaich, 1980: Studies of skeletal remodeling in aging men. Clin. Orthop. Relat. Res. **149,** 268–282.

Michelsen, K., 1967: Pressure relationships in the bone marrow vascular bed. Acta Physiol. Scand. **71,** 16–29.

Mohsin, S., D. Taylor, and T. C. Lee, 2002: Three dimensional reconstruction on Haversian system in ovine compact bone. Eur. J. Morphol. **40,** 309–315.

Pazzaglia, U. E., G. Bonaspetti, L. F. Rodella, F. Ranchetti, and F. Azzola, 2007: Design, morphometry and development of the secondary osteonal system in the femural shaft of the rabbit. J. Anat. **211,** 303–312.

Pazzaglia, U. E., G. Bonaspetti, F. Ranchetti, and P. Bettinsoli, 2008: A model of the intracortical vascular system of long bones and of its organization: an experimental study in rabbit femur and tibia. J. Anat. **213,** 183–193.

Pazzaglia, U. E., T. Congiu, M. Raspanti, F. Ranchetti, and D. Quacci, 2009: Anatomy of the intracortical canal system scanning electron microscopy study in rabbit femur. Clin. Orthop. Relat. Res. **467,** 2446–2456.

Polig, E., and W. S. Jee, 1990: A model of osteon closure in cortical bone. Calcif. Tissue Int. **47,** 261–269.

Richman, E. A., D. J. Ortner, and F. P. Shulter-Ellis, 1979: Differences in intracortical bone remodeling in three aboriginal American populations: possible dietary factors. Calcif. Tissue Int. **28,** 209–214.

Rogers, W. M., and H. Gladstone, 1950: Vascular foramina and arterial supply of distal end of the femur. J. Bone Joint Surg. Am. **32,** 867–874.

Schenk, R., and H. Willenegger, 1964: On the histology of primary bone healing. Langenbecks Arch. Klin. Chir. Ver. Dtsch. Z. Chir. **308,** 955–968.

Shim, S. S., H. F. Hawk, and W.Y. Yu, 1972: The relationship between blood flow and marrow cavity pressure of bone. Surg. Gynec. Obst. **135,** 353–360.

Smith, J. W., 1960: Collagen fibre patterns in mammalian bone. J. Anat. **94,** 329–344.

Smith, J. W., and S. Andrew, 1963: Age changes in the organic fraction of bone. J. Bone Joint Surg. Br. **45,** 761–769.

Stein, A. H., H. C. Morgan, and R. F. Porras, 1958: The effect of pressor and depressor drugs on intramedullary bone-marrow pressure. J. Bone Joint Surg. Am. **40,** 1103–1110.

Stout, S. D., B. S. Brunsden, C. F. Hildebolt, P. K. Commean, K. E. Smith, and N. C. Tappen, 1999: Computer-assisted 3D reconstruction of serial sections of cortical bone to determine the 3D structure of osteons. Calcif. Tissue Int. **65,** 280–284.

Thompson, J. C., 2002: Netter's Concise Atlas of Orthopaedic Anatomy. Teterboro, NY: Multimedia USA Inc.

Trias, A., and A. Fery, 1979: Cortical circulation of long bones. J. Bone Joint Surg. Am. **61,** 1052–1059.

Vasciaveo, F., and E. Bartoli, 1961: Vascular channels and resorption cavities in the long bone cortex the bovine bone. Acta Anat. **47,** 1–33.